Int J Adv Manuf Technol (2017) 92:583–595
DOI 10.1007/s00170-017-0171-y

ORIGINAL ARTICLE

A second-order semi-discretization method for the efficient and accurate stability prediction of milling process

Shanglei Jiang[1] · **Yuwen Sun**[1] · **Xilin Yuan**[1] · **Weirui Liu**[1]

Received: 12 October 2016 / Accepted: 15 February 2017 / Published online: 1 March 2017

Abstract Due to the high computational accuracy and good applicability with a low complexity of algorithm, semi-discretization method has a significant application for predicting milling stability, but to some extent it has some limitations in computational efficiency. Based on the Newton interpolation polynomial and an improved precise time-integration (PTI) algorithm, a second-order semi-discretization method for efficiently and accurately predicting the stability of the milling process is proposed. In the method, the milling dynamic system considering the regenerative effect is first approximated by a time-periodic delayed-differential equation (DDE) and then reformulated in state-space form. After discretizing the time period into a finite number of time intervals, the equation is integrated on each discrete time interval. In order to improve the approximation accuracy of the time-delay item, a second-order Newton interpolation polynomial is utilized instead of a linear function used in the original first-order semi-discretization method (SDM). Next, with a rapid matrix computation technique, an improved precise time-integration algorithm is employed to calculate the resulting exponential matrices efficiently. Finally, transition matrix of the system is constructed over the discretization period and the milling stability boundary is determined by Floquet theory. Compared with the typical discretization methods, the proposed method indicates a faster convergence rate. Further, two benchmark examples are given to validate the effectiveness of the proposed method from the aspects of computational efficiency and accuracy.

Keywords Milling stability · Second-order semi-discretization method · Newton interpolation · Precise time-integration · Floquet theory

1 Introduction

In the cutting operation, due to the intense dynamic periodic interaction between the cutter and workpiece, regenerative chatter, as a very common self-excited vibration, may probably be produced. It inevitably brings some disadvantages in the efficiency and accuracy of cutting and even deteriorates the machined surface quality and the performance of the CNC machine tool [1–3]. Most works, involved in preventing the regenerative chatter in the cutting process, utilize a stability lobe diagram to predict the limits of cutting stability in the cutting parameter space. Therefore, how to get a stability chart with high computational efficiency and accuracy is a key issue to help the machinist choose an appropriate combination of cutting parameters in order to acquire high machining productivity and good work-surface finish. Till now, various methods for predicting milling stability lobes have been proposed, which can be categorized as experimental methods [4] and numerical methods.

Numerical methods for the prediction of cutting stability can be mainly classified into frequency-domain-based methods and time-domain-based methods. Altintas and Budak [5] made a great effort in the first direction; they developed a single-frequency solution (SFS) for predicting milling stability. This method provides a rapid computation of stability lobes in milling. However, it has a relatively low prediction accuracy and fails to predict flip bifurcation [6, 7]

✉ Yuwen Sun
xiands@dlut.edu.cn

[1] Key Laboratory for Precision and Non-Traditional Machining Technology of the Ministry of Education, Dalian University of Technology, Dalian 116024, China

as well as the additional stability domain in the parameter space [6]. To handle the issue, Budak and Altintas [8] presented a multi-frequency solution (MFS) for milling stability prediction, and then Merdol and Altintas [9] extended the MFS by considering both the higher harmonics of tooth passing frequency and the highly intermittent process in low radial immersion milling. Utilizing the above frequency solutions, stability models for ball-end milling, variable pitch cutters, face milling, turning and boring operations were proposed [10–15].

In the other direction, Tlusty and Zaton [16] applied a time-domain method to generate the stability lobes. Campomanes and Altintas [17] presented an improved time-domain model to simulate vibratory cutting conditions at low radial immersion milling. In discrete time domain, Bayly and Mann [18] proposed a temporal finite element analysis (TFEA) for an interrupted cutting process by means of multiple finite time elements, which can be used to predict stability at arbitrary times during the cut. Butcher et al. [19] presented a method based on Chebyshev polynomial to predict the stability in up-milling and down-milling operations. By using shifted Chebyshev polynomials, Yan et al. [20] presented a semi-analytical stability prediction method for thin-walled workpiece milling.

Insperger and Stepan [21] proposed a semi-discretization method (SDM), an important method in discrete time domain, which has been widely used for milling stability prediction and developed from zero-order method [22] to first-order method [23]. This method utilized equidistant time nodes to discretize the tooth passing period and is convenient to take one or compound effects into account. For example, by using SDM, Dombovari et al. [24–26] investigated the stability properties of special tool geometries including variable helix tool with distributed delay and serrated and variable pitch tools with multiple delays. Moradi et al. [27] also utilized SDM in their study where the process damping, structural and cutting force nonlinearities of the peripheral milling process were taken into account. Wan et al. [28] proposed an updated SDM to systematically study the stability of the milling process with multiple delays resulting from cutter run-out and variable pitch, and then extended it to thread milling [29]. More extended applications of SDM can be found in Refs. [30–39]. However, during the numerical calculation of SDMs, a large number of matrix exponential and matrix inversion computations are required owing to that they must be updated in the inner loop when sweeping the cutting parameter space, which leads to some losses in the computational efficiency.

On the other hand, a first-order full-discretization method (1st FDM) was proposed by Ding et al. [40]. Compared with SDM, it is a quite efficient method for milling stability prediction. However, it also has brought some disadvantages in computational accuracy [23]. Lately, more and more studies [41–45] were focused on improving FDM based on high-order interpolation or approximation theory. In the study of Ozoegwu et al. [45], a hyper-third-order FDM based on least squares approximation (LSA) was proposed. They pointed out that the computational accuracy of LSA-based FDM peaks at the fourth order and declines at the fifth order. It indicates that the computational accuracy of FDM is not always being improved with increasing degree of interpolation or approximation. In recent years, many new stability prediction methods for milling operations were put forward. For example, Ding et al. [46] proposed the numerical integration method (NIM). Zhang et al. [47] presented a Simpson method. Wan et al. [48] established a lowest envelop method. Tangjitsitcharoen et al. [49] developed an in-process detection-based method. Yang et al. [50] proposed an exponential force model based on a three-dimensional stability prediction method, and many other newly proposed methods can be seen in Refs. [51–58].

Despite this, it is still necessary to further study the SDM due to its aforementioned significant application in practice. A general form of higher-order semi-discretizations for periodic delayed systems was developed by Insperger et al. [59]. However, it is worth noting that the higher-order SDMs were not extended to the stability problem for milling process. Moreover, there is an obvious increase in computational time when improving the computational accuracy of the SDM with a higher-order method. To simultaneously improve the computational efficiency and accuracy of SDM, this paper presents a second-order SDM (2nd SDM) for milling stability prediction. In the framework of SDM, the time-state term in the proposed method is not discretized and the key point is to handle the time-delay term. In this paper, a second-order Newton interpolation polynomial is used to approximate the time-delay term which leads to a significant improvement in approximation accuracy. The exponential matrices resulting from above approximation process are calculated by an improved precise time-integration (PTI) algorithm. The precise time-integration algorithm was originally proposed by Zhong [60] and extended in [61], which is widely used in structural dynamic analysis. In this paper, the system nature matrix inherits the form of SDM, which brings the possibility and convenience of rapid matrix computation. By taking advantage of its benefit, the PTI algorithm is improved. On this base, a first-order SDM is also proposed in order to facilitate the comparison with the original first-order SDM.

2 Mathematical model of the milling dynamic system

In this section, mathematical models of milling dynamic systems with 1-DOF, 2-DOF and n-DOF are described, respectively.

2.1 Milling dynamic model with 1-DOF

The linear single-delay differential equation with a 1-DOF milling tool can be expressed as [1]

$$m_t\ddot{x}(t) + c_t\dot{x}(t) + k_t x(t) = -wh(t)(x(t)-x(t-T)) \tag{1}$$

Where, m_t is the modal mass, c_t is the modal damping, k_t is the modal stiffness and w is the axial cutting depth. The time-delay T satisfies $T=60/N\Omega$, where N is the number of teeth and Ω is the spindle speed in revolutions per minute. The cutting force coefficient $h(t)$ is defined as

$$h(t) = \sum_{j=1}^{N} g(\phi_j(t))\sin(\phi_j(t))\left[K_t\cos(\phi_j(t)) \;\; + K_n\sin(\phi_j(t))\right] \tag{2}$$

Where, K_t and K_n are, respectively, the tangential and normal direction linearized cutting force coefficients under regenerative effects, and ϕ_j is the angular position of jth tooth which is defined as

$$\phi_j(t) = (2\pi\Omega/60)t + (j-1)2\pi/N \tag{3}$$

The unit step function $g(\phi_j(t))$ is defined as

$$g(\phi_j(t)) = \begin{cases} 1 & \text{if } \phi_{st} < \phi_j(t) < \phi_{ex} \\ 0 & \text{otherwise} \end{cases} \tag{4}$$

Where, ϕ_{st} and ϕ_{ex} are, respectively, the start and exit angles of the jth cutter tooth given as

$$\begin{cases} \text{For up-milling} \begin{cases} \phi_{st} = 0 \\ \phi_{ex} = \arccos(1-2a/D) \end{cases} \\ \text{For down-milling} \begin{cases} \phi_{st} = \arccos(2a/D-1) \\ \phi_{ex} = \pi \end{cases} \end{cases} \tag{5}$$

Where, a/D is the ratio of the radial cutting depth and tool diameter.

By state-space transformation, Eq. (1) can be rewritten in the following form:

$$\dot{\mathbf{X}}(t) = \mathbf{A}(t)\mathbf{X}(t) + \mathbf{B}(\mathbf{t})\mathbf{X}(t-T) \tag{6}$$

Where, $\boldsymbol{A}(t)$ is the system nature matrix and $\boldsymbol{B}(t)$ is the force coefficient matrix, which are periodically varying with time and can be expressed by

$$\mathbf{A}(t) = \begin{bmatrix} 0 & 1 \\ -k_t/m_t - wh(t)/m_t & -c_t/m_t \end{bmatrix} \tag{7}$$

$$\mathbf{B}(t) = \begin{bmatrix} 0 & 0 \\ h(t) & 0 \end{bmatrix} \tag{8}$$

and the time-state vector $\boldsymbol{X}(t)$ is

$$\mathbf{X}(t) = \begin{bmatrix} \dot{x}(t) \\ \ddot{x}(t) \end{bmatrix} \tag{9}$$

2.2 Milling dynamic model from 2- to *n*-DOF

The linear single-delay differential equation of a 2-DOF symmetric milling tool can be expressed in a matrix-vector form [1]

$$\mathbf{M}\ddot{\mathbf{q}}(t) + \mathbf{C}\,\dot{\mathbf{q}}(t) + \mathbf{K}\mathbf{q}(t) = -w\mathbf{H}(t)(\mathbf{q}(t)-\mathbf{q}(t-T)) \tag{10}$$

Where, the modal mass matrix $\boldsymbol{M}$, modal damping matrix $\boldsymbol{C}$, modal stiffness matrix $\boldsymbol{K}$ and the displacement vector $\boldsymbol{q}(t)$, respectively, are

$$\mathbf{M} = \begin{bmatrix} m_t & 0 \\ 0 & m_t \end{bmatrix}, \quad \mathbf{C} = \begin{bmatrix} c_t & 0 \\ 0 & c_t \end{bmatrix}, \quad \mathbf{K} = \begin{bmatrix} k_t & 0 \\ 0 & k_t \end{bmatrix}, \quad \mathbf{q} = \begin{pmatrix} x(t) \\ y(t) \end{pmatrix} \tag{11}$$

and the cutting force coefficient matrix is

$$\mathbf{H}(t) = \begin{bmatrix} h_{xx}(t) & h_{xy}(t) \\ h_{yx}(t) & h_{yy}(t) \end{bmatrix} \tag{12}$$

Where,

$$h_{xx}(t) = \sum_{j=1}^{N} g(\phi_j(t))\sin(\phi_j(t))\left[K_t\cos(\phi_j(t)) \;\; + K_n\sin(\phi_j(t))\right] \tag{13}$$

$$h_{xy}(t) = \sum_{j=1}^{N} g(\phi_j(t))\cos(\phi_j(t))\left[K_t\cos(\phi_j(t)) \;\; + K_n\sin(\phi_j(t))\right] \tag{14}$$

$$h_{yx}(t) = \sum_{j=1}^{N} g(\phi_j(t))\sin(\phi_j(t))\left[-K_t\sin(\phi_j(t)) \;\; + K_n\cos(\phi_j(t))\right] \tag{15}$$

$$h_{yy}(t) = \sum_{j=1}^{N} g(\phi_j(t))\cos(\phi_j(t))\left[-K_t\sin(\phi_j(t)) \;\; + K_n\cos(\phi_j(t))\right] \tag{16}$$

Similarly, Eq. (10) also can be written in the state-space form

$$\dot{\mathbf{X}}_{4\times1}(t) = \mathbf{A}_{4\times4}(t)\mathbf{X}_{4\times1}(t) + \mathbf{B}_{4\times4}(\mathbf{t})\mathbf{X}_{4\times1}(t-T) \tag{17}$$

Where, the system nature matrix $\boldsymbol{A}_{4\times4}(t)$ and the force coefficient matrix $\boldsymbol{B}_{4\times4}(t)$ can be given by

$$\boldsymbol{A}_{4\times4}(t) = \begin{bmatrix} \mathbf{O}_{2\times2} & \mathbf{I}_{2\times2} \\ -\mathbf{M}_{2\times2}{}^{-1}\mathbf{K}_{2\times2} - w\mathbf{M}_{2\times2}{}^{-1}\mathbf{H}_{2\times2}(t) & -\mathbf{M}_{2\times2}{}^{-1}\mathbf{C}_{2\times2} \end{bmatrix} \tag{18}$$

$$\mathbf{B}_{4\times4}(t)=\begin{bmatrix}\mathbf{O}_{2\times2} & \mathbf{O}_{2\times2}\\ w\mathbf{M}_{2\times2}{}^{-1}\mathbf{H}_{2\times2}(t) & \mathbf{O}_{2\times2}\end{bmatrix} \tag{19}$$

and the time-state vector $\boldsymbol{X}(t)$ is

$$\mathbf{X}(t)=\left[x(t)\ y(t)\ \dot{x}(t)\ \dot{y}(t)\right]^T \tag{20}$$

Comparing Eqs. (6) with (17), no matter the 1-DOF or 2-DOF milling model, the system nature matrix $\mathbf{A}(t)$ in both equations has similar elements, so does matrix$\mathbf{B}(t)$ and vector $\mathbf{X}(t)$. The only difference between 1-DOF and 2-DOF milling models is that elements of $\mathbf{A}(t)$, $\mathbf{B}(t)$ and $\mathbf{X}(t)$ are 2×2 submatrices in the 2-DOF milling model. This can be further extended to n-DOF milling model given as

$$\dot{\mathbf{X}}_{2n\times1}(t)=\mathbf{A}_{2n\times2n}(t)\mathbf{X}_{2n\times1}(t)+\mathbf{B}_{2n\times2n}(t)\mathbf{X}_{2n\times1}(t-T) \tag{21}$$

with

$$\mathbf{A}_{2n\times2n}(t)=\begin{bmatrix}\mathbf{O}_{n\times n} & \mathbf{I}_{n\times n}\\ -\mathbf{M}_{n\times n}{}^{-1}\mathbf{K}_{n\times n}-w\mathbf{M}_{n\times n}{}^{-1}\mathbf{H}_{n\times n}(t) & -\mathbf{M}_{n\times n}{}^{-1}\mathbf{C}_{n\times n}\end{bmatrix} \tag{22}$$

$$\mathbf{B}_{2n\times2n}(t)=\begin{bmatrix}\mathbf{O}_{n\times n} & \mathbf{O}_{n\times n}\\ w\mathbf{M}_{n\times n}{}^{-1}\mathbf{H}_{n\times n}(t) & \mathbf{O}_{n\times n}\end{bmatrix} \tag{23}$$

$$\mathbf{X}_{2n\times1}(t)=\left[\mathbf{q}_{n\times1}(t)\quad\dot{\mathbf{q}}_{n\times1}(t)\right]^T \tag{24}$$

Where, $\mathbf{O}_n$ and $\mathbf{I}_n$ are $n\times n$ zero matrix and unit matrix, respectively. $\mathbf{M}_n$, $\mathbf{C}_n$ and $\mathbf{K}_n$ are $n\times n$ modal mass, damping and stiffness matrices, respectively. $\mathbf{H}_n(t)$ is $n\times n$ cutting force coefficient matrix. $\mathbf{q}_{n\times1}(t)$ and $\mathbf{q}_{n\times1}(t)$ are $n\times1$ modal displacement and velocity vectors, respectively.

Without a DOF subscript, Eqs. (17) and (21) are reduced into Eq. (6), which can be regarded as a general and universal form no matter what the number of DOF is.

3 Proposed first-order and two-order SDMs

The dynamical equations (Eq. (6)) of the milling system are periodic time-delayed differential equations which are focused on the dynamic behavior of the tool tip, and thus can be categorized as the single-point contact model. They are solved with the proposed first-order and two-order SDM presented here. The time-delay T is equidistantly divided into m small time intervals satisfying $T=m\tau$, where m is an integer. In original SDMs, system nature matrix $\mathbf{A}(t)$ is approximated by a piecewise constant. Therefore, the procedure of discretizing the time-state term is not needed. This avoids deriving the complex mathematical formula as high-order FDMs [41–45] have done. With retaining the similar way of handling the system nature matrix $\mathbf{A}(t)$ as SDM, Eq. (21) can be integrated in each time interval $k\tau\le t\le(k+1)\tau$ $(k=0,\ \ldots,m)$ as follows:

$$\begin{cases}\mathbf{X}_{k+1}=e^{\mathbf{A}_k\tau}\mathbf{X}_k+\mathbf{DI}\\ \mathbf{DI}=\int_0^\tau e^{\mathbf{A}_k s}\mathbf{B}(k\tau+\tau-s)\mathbf{X}(k\tau+\tau-s-T)ds\end{cases} \tag{25}$$

Where, $\mathbf{A}_k$ is namely the system nature matrix $\mathbf{A}(t)$ at $t=k\tau$. $\mathbf{X}_k$ and $\mathbf{X}_{k+1}$ are, respectively, the time-state vectors of $\mathbf{X}(t)$ at $t=k\tau$ and $t=(k+1)\tau$. **DI** denotes the Duhamel integral in which $\mathbf{B}(*)$ is the periodic-coefficient term and $\mathbf{X}(*)$ is the time-delay term.

3.1 Proposed first-order SDM

In the proposed 1st SDM, linear interpolation is used to approximate periodic-coefficient term $\mathbf{B}(k\tau+\tau-s)$ and time-delay term $\mathbf{X}(k\tau+\tau-s-T)$ as follows:

$$\mathbf{B}(k\tau+\tau-s)\approx\mathbf{B}_{k+1}+\frac{(\mathbf{B}_k-\mathbf{B}_{k+1})s}{\tau} \tag{26}$$

$$\mathbf{X}(k\tau+\tau-s-T)\approx\mathbf{X}_{k+1-m}+\frac{(\mathbf{X}_{k-m}-\mathbf{X}_{k+1-m})s}{\tau} \tag{27}$$

Where, $\mathbf{B}_{k+1}=\mathbf{B}(k\tau+\tau)$, $\mathbf{B}_k=\mathbf{B}(k\tau)$, $\mathbf{X}_{k+1}=\mathbf{X}(k\tau+\tau)$ and$\mathbf{X}_{k+1-m}=\mathbf{X}(k\tau+\tau-m\tau)$.

Substituting Eqs. (26) and (27) into Eq. (25) leads to

$$\mathbf{X}_{k+1}=\mathbf{F}_0\mathbf{X}_k+\mathbf{F}_{m-1}\mathbf{X}_{k+1-m}+\mathbf{F}_m\mathbf{X}_{k-m} \tag{28}$$

Where,

$$\mathbf{F}_0=\mathbf{\Phi}_0 \tag{29}$$

$$\mathbf{F}_{m-1}=\left[(\tau\mathbf{\Phi}_2-\mathbf{\Phi}_3)\mathbf{B}_k+\left(\tau^2\mathbf{\Phi}_1+\mathbf{\Phi}_3-2\tau\mathbf{\Phi}_2\right)\mathbf{B}_{k+1}\right]/\tau^2 \tag{30}$$

$$\mathbf{F}_m=\left[\mathbf{\Phi}_3\mathbf{B}_k+(\tau\mathbf{\Phi}_2-\mathbf{\Phi}_3)\mathbf{B}_{k+1}\right]/\tau^2 \tag{31}$$

and

$$\mathbf{\Phi}_0=e^{\mathbf{A}_k\tau} \tag{32}$$

$$\mathbf{\Phi}_1=\int_0^\tau e^{\mathbf{A}_k s}ds \tag{33}$$

$$\mathbf{\Phi}_2=\int_0^\tau s e^{\mathbf{A}_k s}ds \tag{34}$$

$$\mathbf{\Phi}_3=\int_0^\tau s^2 e^{\mathbf{A}_k s}ds \tag{35}$$

Considering the advantage of high computational efficiency and accuracy, PTI algorithm is employed to calculate the resulting $\mathbf{\Phi}_0$,$\mathbf{\Phi}_1$,$\mathbf{\Phi}_2$ and $\mathbf{\Phi}_3$ without solving any inverse

matrices. The pseudo-codes of the calculations are listed in Table 1. The fundamental detail about PTI algorithm can be obtained from Refs. [60, 61].

Next, according to Eq. (28), a discrete map can be defined as

$$\mathbf{Z}_{k+1} = \mathbf{M}_k \mathbf{Z}_k \tag{36}$$

Where,

$$\mathbf{M}_k = \begin{bmatrix} \mathbf{F}_0 & \mathbf{O} & \cdots & \mathbf{O} & \mathbf{F}_{m-1} & \mathbf{F}_m \\ \mathbf{I} & \mathbf{O} & \cdots & \mathbf{O} & \mathbf{O} & \mathbf{O} \\ \mathbf{O} & \mathbf{I} & \cdots & \mathbf{O} & \mathbf{O} & \mathbf{O} \\ \vdots & \vdots & \ddots & \vdots & \vdots & \vdots \\ \mathbf{O} & \mathbf{O} & \cdots & \mathbf{I} & \mathbf{O} & \mathbf{O} \\ \mathbf{O} & \mathbf{O} & \cdots & \mathbf{O} & \mathbf{I} & \mathbf{O} \end{bmatrix} \tag{37}$$

$$\mathbf{Z}_k = \mathrm{col}(\mathbf{X}_k, \mathbf{X}_{k-1}, \cdots, \mathbf{X}_{k+1-m}\mathbf{X}_{k-m}) \tag{38}$$

Now, the Floquet transition matrix of the milling dynamic system can be constructed over a discretization period T by using the sequence of discrete maps $\boldsymbol{M}_k$ ($k=0, 1, \ldots, m-1$). For example,

$$\mathbf{Z}_m = \mathbf{M}\mathbf{Z}_0 \tag{39}$$

Where,

$$\mathbf{M} = \mathbf{M}_{m-1}\mathbf{M}_{m-2}\ldots\mathbf{M}_1\mathbf{M}_0 \tag{40}$$

Finally, the stability of the milling dynamic system can be determined using the Floquet theory: in the cutting parameter space, the stability lobes can be drawn under the condition where the eigenvalues of Floquet transition matrix $\boldsymbol{M}$ are in modulus equal to 1. The milling process will be stable if a cutting parameter combination is chosen in the lower region of stability lobes; otherwise, it will be unstable.

3.2 Proposed 2nd SDM

In the proposed 2nd SDM, periodic-coefficient term is still approximated by linear interpolation, but the time-delay term is approximated by a second-order Newton interpolation as follows:

$$\mathbf{X}(k\tau + \tau - s - T) \approx a\mathbf{X}_{k+2-m} + b\mathbf{X}_{k+1-m} + c\mathbf{X}_{k-m} \tag{41}$$

Where,

$$a = \frac{s^2}{2\tau^2} - \frac{s}{2\tau} \tag{42}$$

$$b = 1 - \frac{s^2}{\tau^2} \tag{43}$$

$$c = \frac{s^2}{2\tau^2} + \frac{s}{2\tau} \tag{44}$$

Substituting Eqs. (26) and (41) into Eq. (25) leads to

$$\mathbf{X}_{k+1} = \mathbf{F}_0\mathbf{X}_k + \mathbf{F}_{m-2}\mathbf{X}_{k+2-m} + \mathbf{F}_{m-1}\mathbf{X}_{k+1-m} + \mathbf{F}_m\mathbf{X}_{k-m} \tag{45}$$

Where,

$$\mathbf{F}_0 = \boldsymbol{\Phi}_0 \tag{46}$$

$$\mathbf{F}_{m-2} = [\mathbf{L}_1\mathbf{B}_k + (-2\mathbf{L}_1 - \mathbf{L}_2)\mathbf{B}_{k+1}]/2\tau^3 \tag{47}$$

$$\mathbf{F}_{m-1} = [\mathbf{L}_2\mathbf{B}_k + (\mathbf{L}_1 + \mathbf{L}_3)\mathbf{B}_{k+1}]/\tau^3 \tag{48}$$

$$\mathbf{F}_m = [\mathbf{L}_4\mathbf{B}_k + \mathbf{L}_2\mathbf{B}_{k+1}]/2\tau^3 \tag{49}$$

$$\mathbf{L}_1 = \boldsymbol{\Phi}_4 - \tau\boldsymbol{\Phi}_3 \tag{50}$$

$$\mathbf{L}_2 = -\boldsymbol{\Phi}_4 + \tau^2\boldsymbol{\Phi}_2 \tag{51}$$

$$\mathbf{L}_3 = -\tau^2\boldsymbol{\Phi}_2 + \tau^3\boldsymbol{\Phi}_1 \tag{52}$$

$$\mathbf{L}_4 = \boldsymbol{\Phi}_4 + \tau\boldsymbol{\Phi}_3 \tag{53}$$

and

$$\boldsymbol{\Phi}_4 = \int_0^\tau s^3 e^{\mathbf{A}_k s} ds \tag{54}$$

In the same way, $\boldsymbol{\Phi}_0$,$\boldsymbol{\Phi}_1$,$\boldsymbol{\Phi}_2$, $\boldsymbol{\Phi}_3$ and $\boldsymbol{\Phi}_4$ are calculated by using the PTI algorithm and the pseudo-codes of the calculations are listed in Table 2. After $\boldsymbol{\Phi}_0$,$\boldsymbol{\Phi}_1$,$\boldsymbol{\Phi}_2$, $\boldsymbol{\Phi}_3$ and $\boldsymbol{\Phi}_4$are acquired, according to Eq. (45), a discrete map for the second-order SDM can be defined as:

$$\mathbf{Z}_{k+1} = \mathbf{M}_k\mathbf{Z}_k \tag{55}$$

Where,

$$\mathbf{M}_k = \begin{bmatrix} \mathbf{F}_0 & \mathbf{O} & \cdots & \mathbf{F}_{m-2} & \mathbf{F}_{m-1} & \mathbf{F}_m \\ \mathbf{I} & \mathbf{O} & \cdots & \mathbf{O} & \mathbf{O} & \mathbf{O} \\ \mathbf{O} & \mathbf{I} & \cdots & \mathbf{O} & \mathbf{O} & \mathbf{O} \\ \vdots & \vdots & \ddots & \vdots & \vdots & \vdots \\ \mathbf{O} & \mathbf{O} & \cdots & \mathbf{I} & \mathbf{O} & \mathbf{O} \\ \mathbf{O} & \mathbf{O} & \cdots & \mathbf{O} & \mathbf{I} & \mathbf{O} \end{bmatrix} \tag{56}$$

$$\mathbf{Z}_k = \mathrm{col}(\mathbf{X}_k, \mathbf{X}_{k-1}, \cdots, \mathbf{X}_{k+1-m}\mathbf{X}_{k-m}) \tag{57}$$

Similarly, the Floquet transition matrix of the milling dynamic system can be constructed over a discretization period T by using the sequence of discrete maps $\boldsymbol{M}_k$ ($k=0, 1, \ldots, m-1$); for example,

$$\mathbf{Z}_m = \mathbf{M}\mathbf{Z}_0 \tag{58}$$

Where,

$$\mathbf{M} = \mathbf{M}_{m-1}\mathbf{M}_{m-2}\ldots\mathbf{M}_1\mathbf{M}_0 \tag{59}$$

Finally, the stability lobes of the milling dynamic system can be determined using the Floquet theory.

The proposed two solution methods are also applicable to multiple-point contact models [62, 63] which take into account the dynamic behavior of several representative axial contact points at the tool-part contact zone and are more suitable for the stability issues of thin-walled workpiece milling. This is because the dynamical equations of the state-space form in both single-point contact model and multiple-point contact models are similar and their construction procedures of Floquet transition matrix M are the same.

3.3 Rapid matrix computation of the *j*th power of system nature matrix

It can be seen from Tables 1 and 2, during the calculation process of the PTI algorithm, a large amount of *j*th power of system nature matrix needs to be calculated which appears in the form $\boldsymbol{A_k}^i$ $(i=2,3,\ldots)$. On the other hand, it also can be found in Eq. (22) that half of the elements in system nature matrix $\boldsymbol{A_k}$ are zero matrix $\mathbf{O}$ and unit matrix and $\mathbf{I}$. With the help of this particularity, an improvement for PTI algorithm can be achieved by the following recursive formula:

$$\boldsymbol{A_k}^i = \boldsymbol{A_k}\boldsymbol{A_k}^{i-1} = \begin{bmatrix} \mathbf{O}_i & \mathbf{E}_i \\ \mathbf{P}_i & \mathbf{Q}_i \end{bmatrix} = \begin{bmatrix} \mathbf{O} & \mathbf{E} \\ \mathbf{P} & \mathbf{Q} \end{bmatrix} \begin{bmatrix} \mathbf{O}_{i-1} & \mathbf{E}_{i-1} \\ \mathbf{P}_{i-1} & \mathbf{Q}_{i-1} \end{bmatrix} = \begin{bmatrix} \mathbf{P}_{i-1} & \mathbf{Q}_{i-1} \\ \mathbf{P}_i & \mathbf{Q}_i \end{bmatrix} \tag{60}$$

Table 1 The pseudo-codes of calculating $\boldsymbol{\Phi}_0$, $\boldsymbol{\Phi}_1$, $\boldsymbol{\Phi}_2$ and $\boldsymbol{\Phi}_3$

```
1:  Φ0' ⇐ ηA_k + (η^2 A_k^2)/2! + (η^3 A_k^3)/3! + (η^4 A_k^4)/4!
2:  Φ3 ⇐ η^3 (I/3 + ηA_k/4 + (η^2 A_k^2)/10)
3:  for j = 0; j < p; j++ do
4:      Φ2 ⇐ η^2 (I + Φ0') (−A_k × Φ3)/2
5:      Φ1 ⇐ η(I + Φ0') − A_k × Φ2
6:      Φ3 ⇐ Φ3 + (I + Φ0') (Φ3 + 2ηΦ2 + η^2 Φ1)
7:      Φ0' ⇐ 2Φ0' + Φ0' × Φ0'
8:      η ⇐ 2η
9:  end for
10: Φ0 ⇐ I + Φ0'
11: Φ2 ⇐ (η^2 Φ0 − A_k × Φ3)/2
12: Φ1 ⇐ ηΦ0 − A_k × Φ2
```

p is the precision exponent of the PTI algorithm which satisfies $\eta = \tau/2^p$

Table 2 The pseudo-codes of calculating $\boldsymbol{\Phi}_0$, $\boldsymbol{\Phi}_1$, $\boldsymbol{\Phi}_2$, $\boldsymbol{\Phi}_3$ and $\boldsymbol{\Phi}_4$

```
1:  Φ0' ⇐ ηA_k + (η^2 A_k^2)/2! + (η^3 A_k^3)/3! + (η^4 A_k^4)/4!
2:  Φ4 ⇐ η^4 (I/4 + ηA_k/5 + (η^2 A_k^2)/12)
3:  for j = 0; j < p; j++ do
4:      Φ3 ⇐ η^3 (I + Φ0') (−A_k × Φ4)/3
5:      Φ2 ⇐ η^2 (I + Φ0') (−A_k × Φ3)/2
6:      Φ1 ⇐ η(I + Φ0') − A_k × Φ2
7:      Φ4 ⇐ Φ4 + (I + Φ0') (Φ4 + 3ηΦ3 + 3η^2 Φ2 + η^3 Φ1)
8:      Φ0' ⇐ 2Φ0' + Φ0' × Φ0'
9:      η ⇐ 2η
10: end for
11: Φ0 ⇐ I + Φ0'
12: Φ3 ⇐ (η^3 Φ0 − A_k × Φ4)/3
13: Φ2 ⇐ (η^2 Φ0 − A_k × Φ3)/2
14: Φ1 ⇐ ηΦ0 − A_k × Φ2
```

Where,

$$\mathbf{P}_i = \mathbf{P}\mathbf{O}_{i-1} + \mathbf{Q}\mathbf{P}_{i-1} \tag{61}$$

$$\mathbf{Q}_i = \mathbf{P}\mathbf{E}_{i-1} + \mathbf{Q}\mathbf{Q}_{i-1} \tag{62}$$

with

$$\mathbf{O}_{i-1} = \mathbf{P}_{i-2} \tag{63}$$

$$\mathbf{E}_{i-1} = \mathbf{Q}_{i-2} \tag{64}$$

$$\mathbf{P} = -\mathbf{M}^{-1}\mathbf{K} - w\mathbf{M}^{-1}\mathbf{H}(t_k) \tag{65}$$

$$\mathbf{Q} = -\mathbf{M}^{-1}\mathbf{C} \tag{66}$$

$$\mathbf{P}_0 = \mathbf{O}, \quad \mathbf{P}_1 = \mathbf{P}, \quad \mathbf{Q}_0 = \mathbf{I}, \quad \mathbf{Q}_1 = \mathbf{Q}, \tag{67}$$

It is noted in Eq. (60) that half of the elements in matrix $\boldsymbol{A_k}^i$ are the other half of the elements in matrix $\boldsymbol{A_k}^{i-1}$. This leads to a significant reduction of multiplications in millions of loop computations when the program is sweeping the cutting parameter space. As a result, the scale of calculation of $\boldsymbol{\Phi}_n$ $(n=0,1,2,\cdots)$ can be significantly reduced by using the PTI algorithm improved through this rapid matrix computation. Note that the system nature matrix in this paper inherits the form of that in the original SDM, which brings the convenience and possibility of the rapid computation.

Table 3 Milling parameters

Natural frequency	$\omega_n = 922Hz$
Mass	$m = 0.03993$kg
Damping ratio	$\xi = 0.011$
Tangential cutting coefficient	$K_t = 600N/mm^2$
Normal cutting coefficient	$K_n = 200N/mm^2$
Number of teeth	$N = 2$
Precision exponent of PTI algorithm	$p = 2$

4 Convergence analysis

Rate of convergence estimates is normally used in existing literatures [23, 41–47]. It utilizes the local discretization error to estimate the difference between the approximate solution $\mathbf{x}(t)$ and the exact solution $\mathbf{y}(t)$ over a single discretization interval $[0, \tau]$. Namely, the local discretization error is a function of the discretization step τ and defined as $E_{\text{conv}} = \|x(\tau) - y(\tau)\|$. Following the same way, the local discretization error of the proposed 1st and 2nd SDM can be determined as $\mathcal{O}(\tau^3)$.

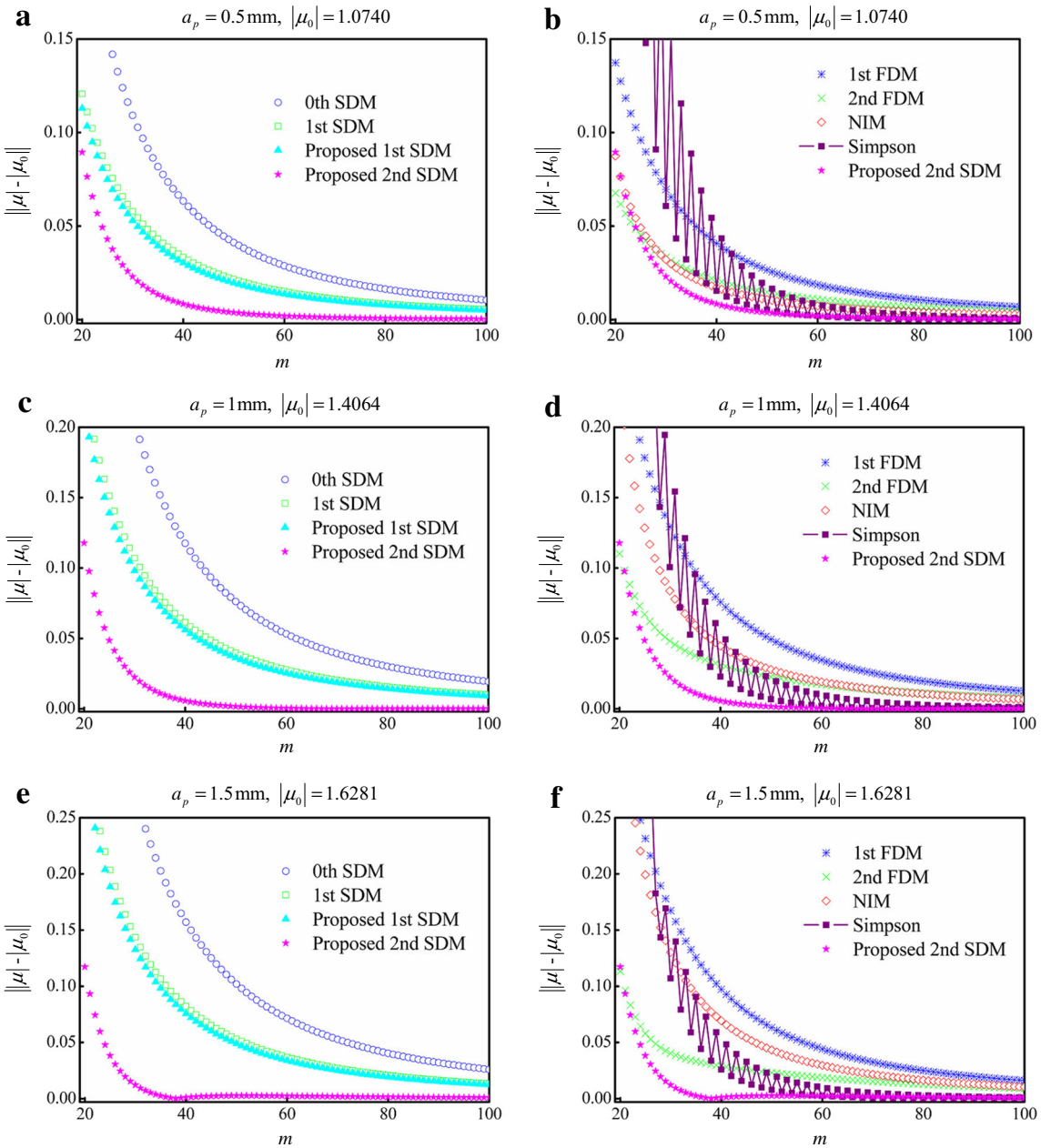

Fig. 1 Convergence of the eigenvalues for the typical methods and proposed methods

Programs are conducted using the Matlab R2014a software on a desktop computer with Intel(R) Core(TM)i5-4430 CPU@3.0 Ghz and 8 GB memory. The modal parameters of the milling dynamic system are chosen as the same as those used in Ref. [23], which are listed in Table 3. The machining parameters are down-milling, the ratio of radial cutting depth and tool diameter $a/D=1$, spindle speed $\Omega=5000$ rpm, three axial cutting depths $a_p=0.5$, 1 and 1.5 mm. In Fig.1, the label $\|\mu_0|-|\mu\|$ of the y-axis represents the deviation between the exact critical eigenvalue μ_0 and the approximate critical eigenvalue μ: where, μ_0 is determined by the original 1st SDM with a large discretization parameter $m=1000$ as reference. It can be proved that if m is large enough, the value of $\|\mu_0|-|\mu\|$ will approach 0 for each method. So, if a method has a faster rate of convergence, the value of $\|\mu_0|-|\mu\|$ will approach 0 more quickly.

Figure 1 shows the convergence curves of different methods. The convergence curves of the original SDMs and the proposed SDMs are illustrated on the left hand side of Fig. 1. Under the same cutting condition, those of the 1st FDM, 2nd FDM, NIM, Simpson method and the proposed 2nd SDM are shown in the same lines of the right hand side. It can be seen from Fig.1a, c and e that the proposed 2nd SDM improves the convergence rate significantly compared with original SDMs. For example, as shown in Fig. 1c, at $m=40$, the value of $\|\mu_0|-|\mu\|$ of the proposed 2nd SDM is already below 5.7×10^{-3}. While those of the 0th SDM and the 1st SDM are 117.4×10^{-3} and 75.7×10^{-3}, respectively, and all of which exceed 5.7×10^{-3} greatly. It also can be found that the proposed 1st SDM converges slightly faster than the original 1st SDM. In Fig. 1b, d and f, the convergence rate of the proposed 2nd FDM is still faster than that of the 1st FDM, the 2nd FDM, the NIM and the newly proposed Simpson method.

5 Effectiveness validation

Under the conditions of low- and high-speed milling operations, two benchmark examples are adopted from the literature [23] to verify the effectiveness of the proposed methods from the aspects of computational efficiency and accuracy for milling stability prediction. Figure 2 shows the computational time and Figs. 3 and 4 show the stability diagrams of different methods.

In order to make a clear comparison, stability lobes are determined by the original 1st SDM with $m=300$, which are marked as an accurate reference stability boundary in red color. The modal parameters of the milling dynamic system have been shown in Table 3. And the machining parameters are down-milling and $a/D=1$.

Case 1: stability prediction in low-speed milling

Stability lobes of widely used 0th–1st SDMs, 1st–2nd FDMs and the proposed 1st–2nd SDMs are presented in Fig. 3 for low-spindle-speed domain with three different discretization parameters $m=50, 70$ and 90. They are calculated over a 200×100-sized grid of the cutting parameters with $\Omega\in[2\times10^3, 2.6\times10^3]$rpm and $w\in[0, 4\times10^{-3}]$m. Their computational time is summarized in Fig. 2a. It can be seen from Fig. 2a that both of the proposed 1st SDM and 2nd SDM spend much less computational time than original SDMs. For example, at $m=70$, the computational time of the original 1st SDM is 328 s, while that of the proposed 1st SDM is 105 s with a 68% reduction and that of the proposed 2nd SDM is 113 s with a 65% reduction. Compared with the 0th SDM which spends 219 s, the reduction ratios of the proposed 1st SDM and 2nd SDM are 52 and 48%, respectively. It means that both of the proposed methods have much higher computational efficiencies than those of the original 1st SDM. And compared with that of the 0th SDM, they still have higher computational efficiencies for milling stability prediction in low-speed milling. It can also be seen from Fig. 2a that even compared with the highly efficient FDMs, the proposed methods still have near computational time only with a slight increase.

In terms of computational accuracy, as shown in Fig. 3, stability lobes of the proposed 2nd SDM have

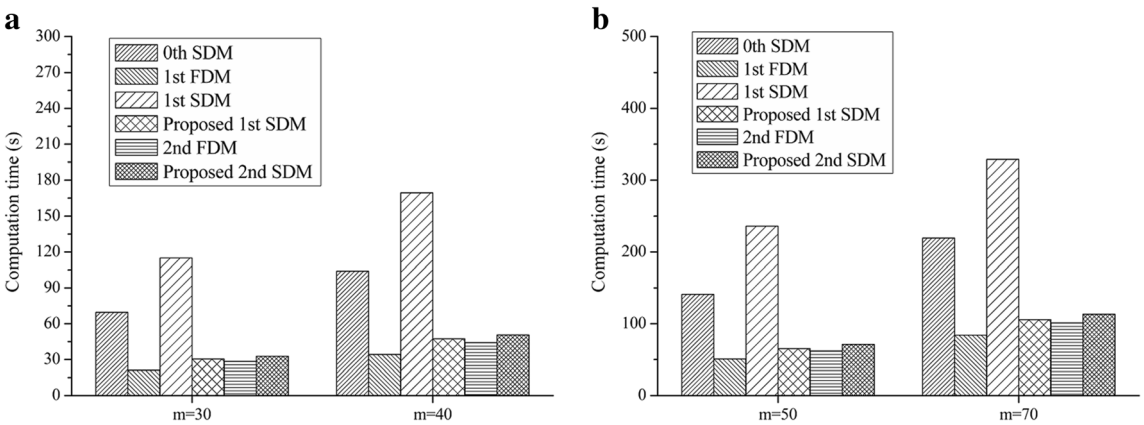

Fig. 2 A comparison of computational time for 0th–1st SDMs, 1st–2nd FDMs and the proposed 1st–2nd SDMs in **a** low-spindle-speed domain and **b** high-spindle-speed domain

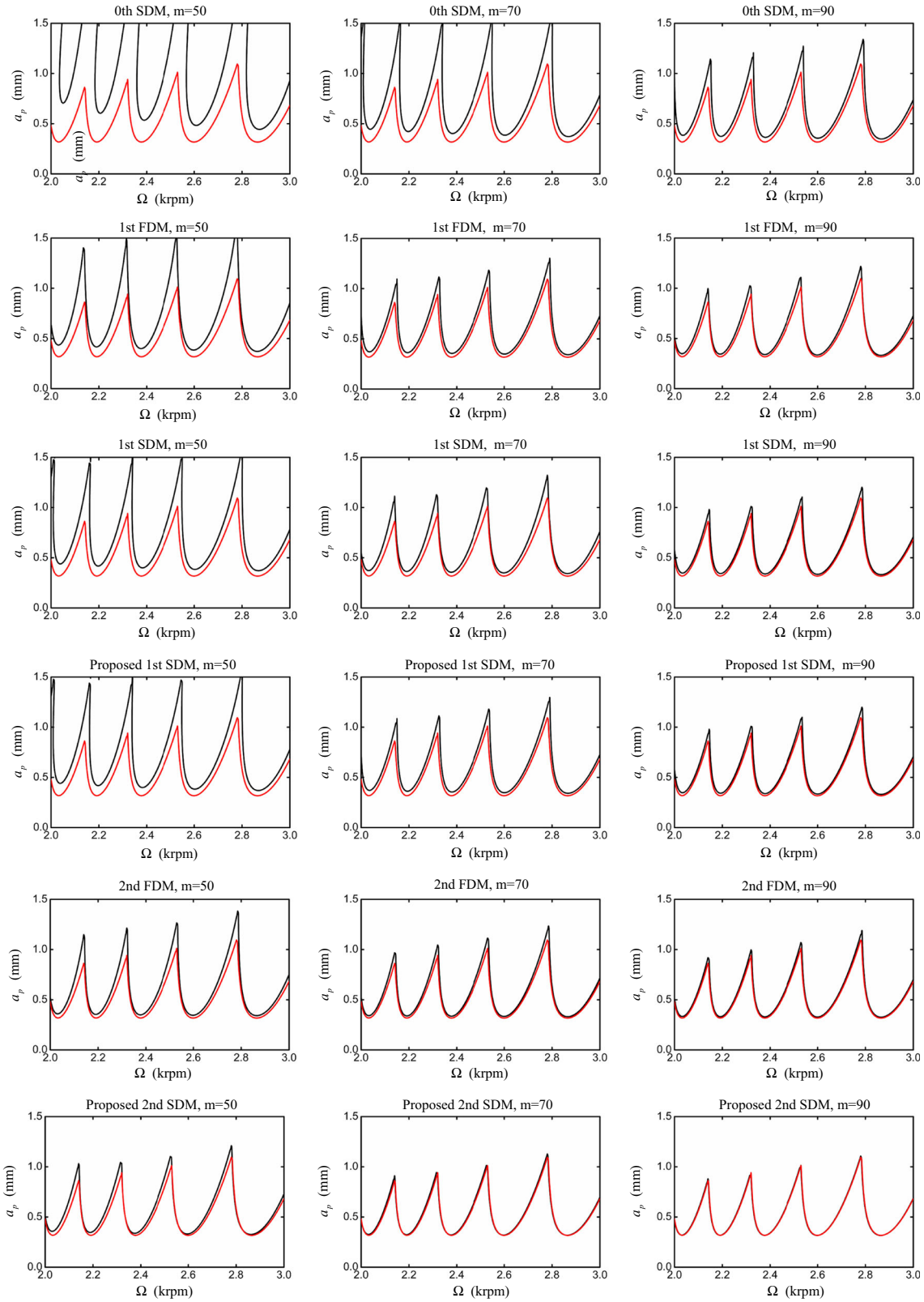

Fig. 3 A comparison of computational accuracy for 0th–1st SDMs, 1st–2nd FDMs and the proposed 1st–2nd SDMs in the low-spindle-speed domain. The stability boundary determined by the original 1st SDM with m=300 is marked in *red color* for reference

much better agreements with the reference stability boundary than those of other methods. For example, at $m = 70$, the stability lobes of the 0th SDM have noticeable deviations from the reference stability boundary,

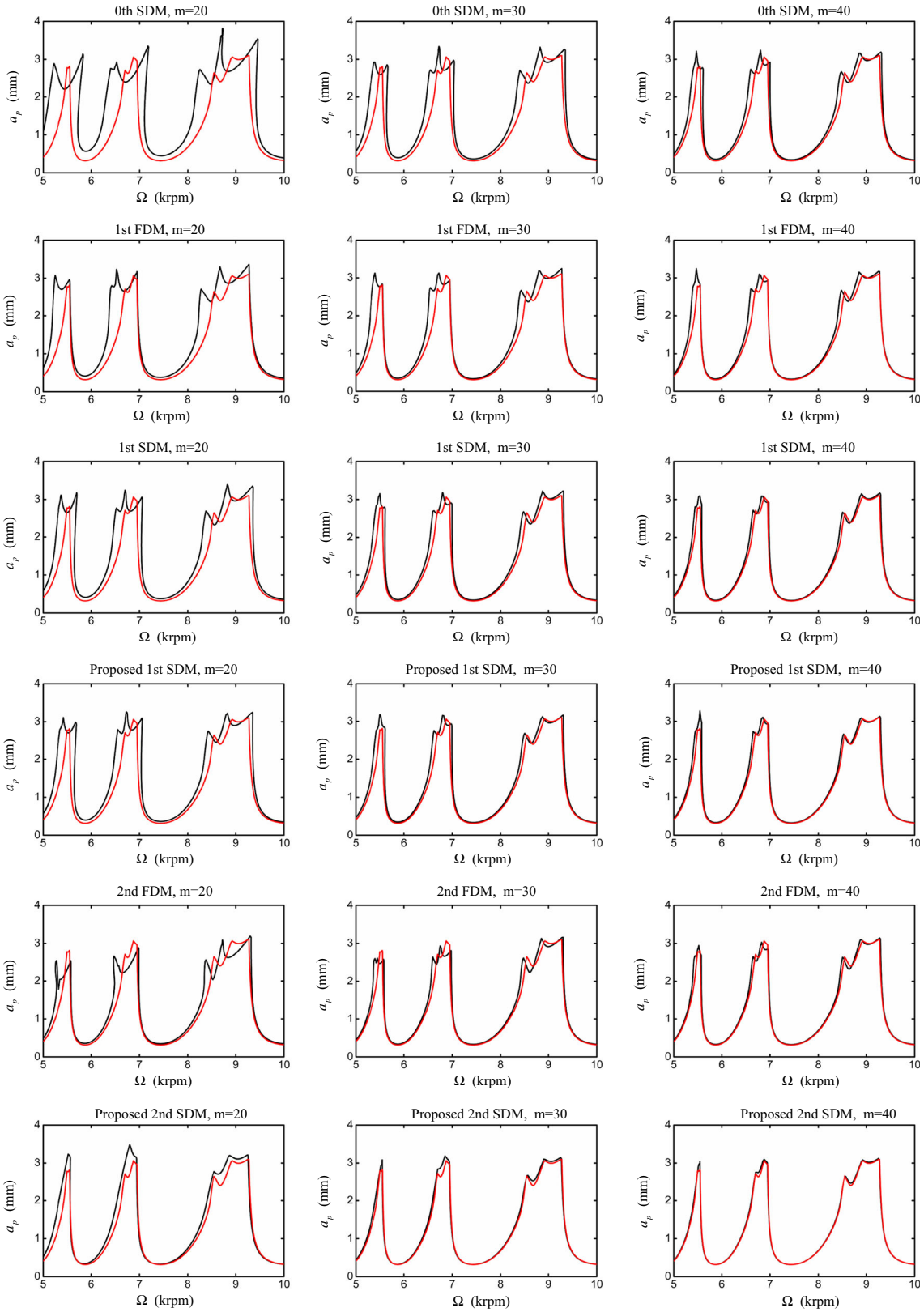

Fig. 4 A comparison of computational accuracy for 0th–1st SDMs, 1st–2nd FDMs and the proposed 1st–2nd SDMs in the high-spindle-speed domain. The stability boundary determined by the original 1st SDM with m=300 is marked in *red color* for reference

especially at the top regions of two adjacent lobes. Although the deviations are further reduced by the original 1st SDM and 2nd FDM, there still exists a visible difference from the reference stability boundary. When using the proposed 2nd SDM, the stability lobes almost coincide with the reference stability boundary. It further indicates that the proposed 2nd SDM has a higher computational accuracy than the other methods in low-speed milling.

Case 2: Stability prediction in high-speed milling

Stability lobes of 0th–1st SDMs, 1st–2nd FDMs and the proposed 1st–2nd SDMs are presented in Fig. 4 for high-spindle-speed domain with three different discretization parameters $m = 20, 30$ and 40. They are calculated over a 200×100-sized grid of the cutting parameters with $\Omega \in [5 \times 10^3, 10 \times 10^3]$rpm and $w \in [0, 1.5 \times 10^{-3}]$m. Their computational time is summarized in Fig. 2b. It can be seen from Fig. 2b that both of the proposed 1st SDM and 2nd SDM still spend much less computational time than the original SDMs. For example, at $m = 30$, the computational time of the original 1st SDM is 115 s, while that of the 1st SDM is 30 s with a 74% reduction and that of the 2nd SDM is 32 s with a 72% reduction. Compared with the 0th SDM which spends 70 s, the reduction ratios of the proposed 1st SDM and 2nd SDM are, respectively 57 and 54%. It means that in high-spindle-speed domain, both of the proposed 1st SDM and 2nd SDM still have much higher computational efficiencies than the original 1st SDM. And compared with that of the 0th SDM, they still have higher computational efficiencies for milling stability prediction in the high-speed milling. It can also be seen from Fig. 2b that even compared with the high-efficiency FDMs, the proposed methods still have near computational time.

In terms of computational accuracy, as shown in Fig. 4, stability lobes of the proposed 2nd SDM still agree most with the reference stability boundary among all the methods. For example, at a small discretization parameter $m = 20$, obvious deviations can be found between the stability lobes of 0th SDM and the reference stability boundary. Although the deviations are further reduced by the original 1st SDM and 2nd FDM, there still exists a visible difference from the reference stability boundary. When using the proposed 2nd SDM, the stability lobes well agree with the reference stability boundary. It further indicates that the proposed 2nd SDM has a higher computational accuracy than other methods in high-speed milling.

6 Conclusions and future works

Based on the Newton interpolation polynomial and an improved PTI algorithm, a second-order SDM is proposed for the milling stability prediction. From this study, the following conclusions can be drawn:

- Instead of using a linear function in the original first-order SDM, a second-order Newton interpolation polynomial is utilized to approximate the time-delay term, which effectively improves the approximation accuracy.
- With the help of a rapid matrix computation technique, an improved precise time-integration algorithm is used to calculate the resulting exponential matrices, which does not need to solve any inverse matrices and effectively reduces the computation time.
- Convergence analysis shows that the proposed second-order SDM improved the convergence rate of original SDMs greatly and also converges faster than the first-order FDM, the second-order FDM, the NIM and the newly proposed Simpson method.
- In terms of computational efficiency, compared with that of the original 0th–1st SDMs, the proposed 2nd SDM reduces the computational time significantly. Compared with that of the 2nd FDM, it has a quite near computational efficiency, while it is just a litter slower in computation time.
- In terms of computational accuracy, the second proposed method has a better agreement with the reference stability boundary than the 0th–1st SDMs and 1st–2nd FDMs using a smaller number of discretization parameters.

In summary, the proposed method is effective and has some remarkable characteristics. In addition, the proposed method has the potential to be used for the chatter stability prediction in milling thin-walled workpiece and difficult-to-cut materials including process damping [64–67], nonlinear force, complex time-delay, et al. However, it needs future research.

Acknowledgments This research is supported by the NSFC (Grant No.51525501, 11290143), SCP (Grant No. JCKY2016212A506-0102) and NSFC (Grant No. 51621064).

References

1. Altintas Y (2012) Manufacturing automation, 2nd edn. Cambridge University Press, Cambridge
2. Tobias SA (1965) Machine tool vibration. Blackie and Sons Ltd, New York

3. Li ZJ, Fang FZ, Gong H, Zhang XD (2013) Review of diamond-cutting ferrous metals. Int J Adv Manuf Technol 68(5–8):1717–1731
4. Quintana G, Ciurana J, Teixidor D (2008) A new experimental methodology for identification of stability lobes diagram in milling operations. Int J Mach Tools Manuf 48(15):1637–1645
5. Altintas Y, Budak E (1995) Analytical prediction of stability lobes in milling. CIRPAnn Manuf Technol 44(1):357–362
6. Bayly PV, Mann BP, Schmitz TL, Peters DA, Stepan G and Insperger T (2002) Effects of radial immersion and cutting direction on chatter instability in end milling. In ASME 2002 International Mechanical Engineering Congress and Exposition, American Society of Mechanical Engineers pp: 351–363
7. Stepan G, Szalai R, Mann BP, Bayly PV, Insperger T, Gradisek J, Govekar E (2005) Nonlinear dynamics of high-speed milling—analyses, numerics, and experiments. J Vib Acoust 127(2):197–203
8. Budak E, Altintas Y (1998) Analytical prediction of chatter stability in milling —part I: general formulation. J Dyn Syst 120(1):22–30
9. Merdol SD, Altintas Y (2004) Multi-frequency solution of chatter stability for low immersion milling. J Manuf Sci Eng 126(3):459–466
10. Altintas Y, Shamoto E, Lee P, Budak E (1999) Analytical prediction of stability lobes in ball end milling. J Manuf Sci Eng 121(4):586–592
11. Altıntaş Y, Engin S, Budak E (1999) Analytical stability prediction and design of variable pitch cutters. J Manuf Sci Eng 121(2):173–178
12. Jensen SA, Shin YC (1999) Stability analysis in face milling operations, part 1: theory of stability lobe prediction. J Manuf Sci Eng 121(4):600–605
13. Jensen SA, Shin YC (1999) Stability analysis in face milling operations, part 2: experimental validation and influencing factors. J Manuf Sci Eng 121(4):606–614
14. Ozlu E, Budak E (2007) Analytical modeling of chatter stability in turning and boring operations—part I: model development. J Manuf Sci Eng 129(4):726–732
15. Ozlu E, Budak E (2007) Analytical modeling of chatter stability in turning and boring operations—part II: experimental verification. J Manuf Sci Eng 129(4):733–739
16. Tlusty J, Zaton W, Ismail F (1983) Stability lobes in milling. CIRP Annals-Manuf Technol 32(1):309–313
17. Campomanes ML, Altintas Y (2003) An improved time domain simulation for dynamic milling at small radial immersions. J Manuf Sci Eng 125(3):416–422
18. Bayly PV, Halley JE, Mann BP, Davies MA (2003) Stability of interrupted cutting by temporal finite element analysis. J Manuf Sci Eng 125(2):220–225
19. Butcher EA, Nindujarla P and Bueler E (2005) Stability of up-and down-milling using Chebyshev collocation method. In ASME 2005 International Design Engineering Technical Conferences and Computers and Information in Engineering Conference, American Society of Mechanical Engineers pp: 841–850
20. Yan Z, Liu Z, Wang X, Liu B, Luo Z and Wang D (2016) Stability prediction of thin-walled workpiece made of Al7075 in milling based on shifted Chebyshev polynomials. Int J Adv Manuf Technol pp:1–10
21. Insperger T, Stepan G (2002) Semi-discretization method for delayed systems. Int J Numer Methods Biomed Eng 55(5):503–518
22. Insperger T, Stépán G (2004) Updated semi-discretization method for periodic delay-differential equations with discrete delay. Int J Numer Methods Eng 61(1):117–141
23. Insperger T (2010) Full-discretization and semi-discretization for milling stability prediction: some comments. Int J Mach Tools Manuf 50(7):658–662
24. Dombovari Z, Stepan G (2012) The effect of helix angle variation on milling stability. J Manuf Sci Eng 134(5):051015
25. Dombovari Z, Munoa J, Stepan G (2012) General milling stability model for cylindrical tools. Procedia CIRP 4:90–97
26. Dombovari Z, Altintas Y, Stepan G (2010) The effect of serration on mechanics and stability of milling cutters. J Manuf Sci Eng 50(6):511–520
27. Moradi H, Vossoughi G, Movahhedy MR (2013) Experimental dynamic modelling of peripheral milling with process damping, structural and cutting force nonlinearities. J Sound Vib 332(19): 4709–4731
28. Wan M, Zhang WH, Dang JW, Yang Y (2010) A unified stability prediction method for milling process with multiple delays. Int J Mach Tools Manuf 50(1):29–41
29. Wan M, Altintas Y (2014) Mechanics and dynamic of thread milling process. Int J Mach Tools Manuf 87:16–26
30. Insperger T, Stepan G (2011) Semi-discretization for time-delay systems: stability and engineering applications. Springer, NewYork
31. Seguy S, Insperger T, Arnaud L (2010) On the stability of high-speed milling with spindle speed variation. Int J Adv Manuf Technol 48:883–895
32. Hartung F, Insperger T, Stépán G, Turi J (2006) Approximate stability charts for milling processes using semi-discretization. Appl Math Comput 174(1):51–73
33. Xie Q, Zhang Q (2012) Stability predictions of milling with variable spindle speed using an improved semi-discretization method. Math Comput Simulat 85:78–89
34. Elías-Zúñiga A, Pacheco-Bolívar J, Araya F, Martínez-López A, Martínez-Romero O, Rodríguez CA (2009) Stability predictions for end milling operations with a nonlinear cutting force model. J Manuf Sci Eng 131(6):064504
35. Ahmadi K, Ismail F (2011) Analytical and stability lobes including nonlinear process damping effect on machining chatter. Int J Mach Tools Manufacture 51(4):296–308
36. Ahmadi K, Ismail F (2012) Modeling chatter in peripheral milling using the semi discretization method. CIRP Annals-Manuf Technol 5(2):77–86
37. Zatarain M, Munoa J, Peigné G, Insperger T (2006) Analysis of the influence of mill helix angle on chatter stability. CIRP Annals-Manuf Technol 55(1):365–368
38. Insperger T, Gradišek J, Kalveram M, Stépán G, Winert K, Govekar E (2006) Machine tool chatter and surface location error in milling processes. J Manuf Sci Eng 128(4):913–920
39. Dong XF, Zhang WM, Deng S (2015) The reconstruction of a semi-discretization method for milling stability prediction based on Shannon standard orthogonal basis. Int J Adv Manuf Technol pp: 1–11
40. Ding Y, Zhu LM, Zhang XJ, Ding H (2010) A full-discretization method for prediction of milling stability. Int J Mach Tools Manuf 50(5):502–509
41. Ding Y, Zhu LM, Zhang XJ, Ding H (2010) Second-order full-discretization method for milling stability prediction. Int J Mach Tools Manuf 50(10):926–932
42. Quo Q, Sun YW, Jiang Y (2012) On the accurate calculation of milling stability limits using third-order full-discretization method. Int J Mach ToolsManuf 62:61–66
43. Liu Y, Zhang D, Wu B (2012) An efficient full-discretization method for prediction of milling stability. Int J Mach Tools Manuf 63:44–48
44. Ozoegwu CG (2014) Least squares approximated stability boundaries of milling process. Int J Mach Tools Manuf 79:24–30
45. Ozoegwu CG, Omenyi SN, Ofochebe SM (2015) Hyper-third order full-discretization methods in milling stability prediction. Int J Mach Tools Manuf 92:1–9
46. Ding Y, Zhu LM, Zhang XJ, Ding H (2011) Numerical integration method for prediction of milling stability. J Manuf Sci Eng 133(3): 031005
47. Zhang Z, Li HG, Meng G, Liu C (2015) A novel approach for the prediction of the milling stability based on the Simpson method. Int J Mach Tools Manuf 99:43–47

48. Wan M, Ma YC, Zhang WH, Yang Y (2015) Study on the construction mechanism of stability lobes in milling process with multiple modes. Int J Adv Manuf Technol 79:589–603
49. Tangjitsitcharoen S, Pongsathornwiwat N (2013) Development of chatter detection in milling processes. Int J Adv Manuf Technol 65: 919–927
50. Yang YQ, Liu Q, Zhang B (2014) Three-dimensional chatter stability prediction of milling based on the linear and exponential cutting force model. Int J Adv Manuf Technol 72:1175–1185
51. Tang X, Peng F, Yan R, Gong Y, Li Y and Jiang L. (2016). Accurate and efficient prediction of milling stability with updated full-discretization method. Int J Adv Manuf Technol pp:1–12
52. Jin X, Sun Y, Guo Q, Guo D (2016) 3D stability lobe considering the helix angle effect in thin-wall milling. Int J Adv Manuf Technol 82(9–12):2123–2136
53. Guo Q, Jiang Y, Zhao B, Ming P (2016) Chatter modeling and stability lobes predicting for non-uniform helix tools. Int J Adv Manuf Technol pp:1–16
54. Zhang X, Xiong C, Ding Y and Ding H (2016) Prediction of chatter stability in high speed milling using the numerical differentiation method. Int J Adv Manuf Technol pp:1–10
55. Zhang X, Zhang J, Pang B, Wu D, Zheng X, Zhao W (2016) An efficient approach for milling dynamics modeling and analysis with varying time delay and cutter runout effect. Int J Adv Manuf Technol pp:1–16
56. Xie Q (2016) Milling stability prediction using an improved complete discretization method. Int J Adv Manuf Technol 83(5–8):815–821
57. Q. Guo, Y. Sun, Y. Jiang, Y. Yan, and P. Ming 2016 Determination of the stability lobes with multi-delays considering cutters helix angle effect for machining process, Proc. Inst. Mech. Eng. Part B J. Eng. Manuf
58. Z. Li, Y. Sun, and D. Guo 2016 Chatter prediction utilizing stability lobes with process damping in finish milling of titanium alloy thin-walled workpiece, Int. J. Adv. Manuf. Technol
59. Insperger T, Stépán G, Turi J (2008) On the higher-order semi-discretizations for periodic delayed systems. J Sound Vib 313(1–2):334–341
60. Zhong WX, Williams FW (1994) A precise time step integration method. Proceedings of the Institution of Mechanical Engineers. Part C: J Mech Eng Sci 208(6):427–430
61. Tan S, Zhong W (2007) Precise integration method for Duhamel terms arising from non-homogenous dynamic systems. Chinese Journal of Theoretical and Applied Mechanics 39(3):374–381
62. Eksioglu C, Kilic ZM, Altintas Y (2012) Discrete-time prediction of chatter stability, cutting forces, and surface location errors in flexible milling systems. J Manuf Sci Eng 134(6):61006
63. Yang Y, Zhang WH, Ma YC, Wan M (2016) Chatter prediction for the peripheral milling of thin-walled workpieces with curved surfaces. Int J Mach Tools Manuf 109:36–48
64. Budak E, Tunc LT (2009) A new method for identification and modeling of process damping in machining. J Manuf Sci Eng 131(5):51019
65. Ahmadi K, Altintas Y (2014) Identification of machining process damping using output-only modal analysis. ASME J Manuf Sci Eng 136(c):1–56
66. Wan M, Ma YC, Feng J, Zhang WH (2016) Study of static and dynamic ploughing mechanisms by establishing generalized model with static milling forces. Int J Mech Sci 114:120–131
67. Altintas Y, Eynian M, Onozuka H (2008) Identification of dynamic cutting force coefficients and chatter stability with process damping. CIRP Ann—Manuf Technol 57(1):371–374